

## DECLARATION

I hereby declare that this thesis, entitled **“FABRICATION AND CHARACTERIZATION OF PEROVSKITE SOLAR CELLS AND PERFORMANCE ANALYSIS USING THEORETICAL STUDY,”** is a genuine record of research conducted by me under the supervision and guidance of **Dr. Suman Chatterjee**, Professor, Department of Physics, University of North Bengal, West Bengal. This work is submitted for the award of the degree of **Doctor of Philosophy in Physics**. I also affirm that no part of this thesis has been previously submitted for the award of any other degree or diploma at any other university. Additionally, this thesis has been thoroughly checked for originality using Drillbit plagiarism detection software.

Place: Siliguri

Date: 05.08.2024

*Joy Sarkar*

(Joy Sarkar)

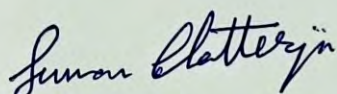
Department of Physics

University of North Bengal

Siliguri- 734013, West Bengal, India

## CERTIFICATE FROM SUPERVISOR

This is to certify that the thesis titled "**FABRICATION AND CHARACTERIZATION OF PEROVSKITE SOLAR CELLS AND PERFORMANCE ANALYSIS USING THEORETICAL STUDY**" is an original piece of research work carried out by **Mr. Joy Sarkar** under my supervision and guidance at the **Department of Physics**, University of North Bengal, West Bengal. This submission is for the degree of **Doctor of Philosophy** in **Physics**. I also confirm that no part of this thesis has been previously submitted for any other degree or diploma at any other institution.



(Dr. Suman Chatterjee)

Professor

Department of Physics

University of North Bengal

Siliguri- 734013, West Bengal, India

Place: *Siliguri.*

Date: *5/8/24*

Professor  
Department of Physics  
University of North Bengal



The Report is Generated by DrillBit Plagiarism Detection Software

**Submission Information**

Author Name Joy Sarkar  
 Title FABRICATION AND CHARACTERIZATION OF PEROVSKITE SOLAR CELLS AND PERFORMANCE ANALYSIS USING THEORETICAL STUDY  
 Paper/Submission ID 2165915  
 Submitted by nbuplg@nbu.ac.in  
 Submission Date 2024-07-25 16:30:24  
 Total Pages, Total Words 260, 63827  
 Document type Thesis

**Result Information**

Similarity 0 %

**Exclude Information**

Quotes Excluded  
 References/Bibliography Excluded  
 Source: Excluded < 14 Words Excluded  
 Excluded Source 4 %  
 Excluded Phrases Not Excluded

**Database Selection**

Language English  
 Student Papers Yes  
 Journals & publishers Yes  
 Internet or Web Yes  
 Institution Repository Yes

Joy Sarkar  
05/08/2024

Signature OR View/Download Sign PDF File  
Suman Chatterjee  
5/8/24

Signature  
5/8/24



Professor  
Department of Physics  
University of North Bengal

HEAD  
Department of Physics  
North Bengal University



### DrillBit Similarity Report

0

SIMILARITY %

0

MATCHED SOURCES

A

GRADE

A-Satisfactory (0-10%)  
B-Upgrade (11-40%)  
C-Poor (41-60%)  
D-Unacceptable (61-100%)

LOCATION      MATCHED DOMAIN      %      SOURCE TYPE

### EXCLUDED SOURCES

1	Thesis Submitted to Shodhganga Repository	1	Publication
2	Thesis submitted to shodhganga - shodhganga.inflibnet.ac.in	<1	Publication
5	www.dx.doi.org	<1	Publication
6	link.springer.com	<1	Internet Data
7	repositorio.uchile.cl	<1	Publication
8	www.mdpi.com	<1	Internet Data
9	Thesis submitted to shodhganga - shodhganga.inflibnet.ac.in	<1	Publication
12	Thesis Submitted to Shodhganga, shodhganga.inflibnet.ac.in	<1	Publication
13	scholarsarchive.library.albany.edu	<1	Publication
15	Exploring electronic and optical properties of Ge-based perovskites un by Sa-2020	<1	Publication
16	pubs.acs.org	<1	Internet Data
17	Thesis Submitted to Shodhganga Repository	<1	Publication
18	link.springer.com	<1	Internet Data

*This thesis is dedicated to my family, especially my  
mother, Archana Sarkar, my brother, Jayanta  
Sarkar, and in loving memory of my father  
Joydeb Chandra Sarkar*

## Preface

Photovoltaic technologies have emerged as a forefront research area in the quest for sustainable energy solutions. As one of the most potent renewable alternatives to fossil fuels, photovoltaics offers the promise of clean, abundant energy through the direct conversion of solar radiation into electricity. While conventional silicon-based solar cells have demonstrated significant potential in harnessing solar energy, their high costs with complex fabrication methods have hindered widespread adoption and competitiveness with traditional power generation methods. In contrast, perovskite solar cells (PSCs) have captivated the scientific community and industry with their remarkable characteristics. These non-conventional photovoltaic technologies stand out due to their exceptional power conversion efficiencies, cost-effectiveness, and the use of recyclable materials. This thesis, titled "**FABRICATION AND CHARACTERIZATION OF PEROVSKITE SOLAR CELLS AND PERFORMANCE ANALYSIS USING THEORETICAL STUDY**," delves into the innovative landscape of PSCs. It investigates the complex procedures of fabricating these cells, rigorously evaluates their performance through detailed characterization, and employs theoretical models to uncover insights that drive further advancements in this field.

This thesis is structured into several key sections. **Chapter 1** offers a comprehensive review of existing literature, emphasizing current developments and challenges in the advancement of perovskite solar cells. This chapter also explores various generations of photovoltaic technology, providing a brief introduction to the components and working principles of perovskite solar cells. **Chapter 2** outlines the theory and working of the various experimental techniques employed to characterize the several components that comprise perovskite solar cells. **Chapter 3** provides an in-depth exploration of the theoretical frameworks and modeling tools utilized to analyze and interpret the performance of perovskite solar cells. **Chapter 4** explores a novel fabrication technique for enhancing the device performance of  $\text{CH}_3\text{NH}_3\text{SnI}_3$ -based perovskite solar cells, focusing on the strategic utilization of a DMSO and activated carbon powder mixture as a counter electrode. **Chapter 5** theoretically examines the impact of Br-substitution on band gap broadening, followed by a detailed theoretical

analysis (based on DFT and SCAPS-1D modeling) of the device performance of lead-free inorganic Ge-based perovskite solar cells. **Chapter 6** studied the effect of metal (Cr, Sr, Ag, and Cu) doping on the performance of all-inorganic Sn-based perovskite solar cells theoretically. **Chapter 7** provides a comprehensive exploration of the fabrication and characterization methods employed to investigate the performance of CsSnI<sub>3</sub>/CsSnBr<sub>3</sub> heterostructure perovskite solar cells. The experimental findings are substantiated through theoretical analysis utilizing Density Functional Theory (DFT). Finally, the essential findings of this study have been outlined in **Chapter 8**.

*Joy Sarkar*

(Joy Sarkar)

Place: Siliguri

Date: 05/08/2024

Department of Physics

University of North Bengal

Siliguri- 734013, West Bengal, India

## Acknowledgements

*There are so many people whose support, encouragement, and inspiration are necessary to accomplish any significant achievements in life, especially if they involve the elements of fulfilling one's cherished dreams. For me, this thesis is such an important destiny, and I am indeed indebted to many people for their wishes and blessings while completing this journey. I take this opportunity to acknowledge and extend my sincere gratitude to all these people who have been involved, directly or indirectly, in making the research work described in this thesis possible.*

*I would like to express my deep and sincere gratitude to Prof. Suman Chatterjee, my Ph.D. supervisor, for permitting me to conduct research under his supervision and providing invaluable support and guidance throughout the endeavor. His vision, commitment, patience, and immense knowledge have significantly influenced me. He has always instructed me on how to present my research work as clearly and concisely as possible. It was a great privilege to work and study under his guidance. Without his constant guidance and support, this research work would not have been accomplished.*

*I am deeply grateful to Prof. Pradip Kumar Mandal, Dept. of Physics, University of North Bengal, for his continuous support, fruitful discussion, encouragement, and sustained help in performing the research work.*

*I sincerely thank the Department of Science and Technology (DST), Government of India, for providing the INSPIRE fellowship (INSPIRE Grant. No. IF180331) and the Department of Physics for providing infrastructural facilities to pursue the research work.*

*My heartfelt thanks to my seniors and fellow labmates, Dr. Rajat Biswas, Pratik Debnath, Avijit Talukdar, Tanmay Chaki, Md Sayeed Sujon, and Subham Subba for stimulating discussions and creating an excellent research environment within the lab.*

*I would like to extend my thanks to all of my colleagues, Dr. Anirban Chanda, Dr. Sagar Dey, Smriti Mitra, Joydeep Thakur, Koushik Chakraborty, and Proloy Halder, for their accompany in the least and the worst time during my research period.*

*I extend my heartfelt gratitude to my friends cum well-wishers Dr. Pronoy Dutta, Dr. Bikash Saha, Anirban Das, Shuvankar Das, Golam Masud Karim, and Subhadeep Roy for their unwavering support and invaluable assistance throughout my research journey.*

*I want to acknowledge all the faculty members and non-teaching staff of the Department of Physics, University of North Bengal, for their needful help during the entire period of my research work. I also extend my heartfelt thanks to the University Science and Instrumentation Centre (USIC) for granting access to their scanning electron microscopy setup, the Department of Chemistry for their support with UV-Vis and PL spectra experiments, the Department of Pharmaceutical Technology at NBU for their assistance with the FTIR study, and finally, IISc Bengaluru for facilitating additional essential experiments.*

*This journey would not have been possible without the enduring love and support of my late father and my beloved Thamma (grandmother), whose memories continue to inspire and guide me. I am eternally grateful for their presence in my life. As I reach this milestone, I hope they are looking down upon me, blessing and celebrating this achievement with me. This accomplishment is a tribute to their enduring legacy in my life. Thank you for always believing in me and being my guiding stars. Finally, I would like to extend my heartfelt gratitude to my entire family, including my Maa, Kaku, Kaki, all my brothers, sisters, and Tupur (my nephew). Their unwavering support made this journey much more bearable and meaningful.*

***Joy Sarkar***

## List of Abbreviations and Symbols

CB	Conduction band
PSC	Perovskite Solar cell
DSSC	Dye-sensitized solar cell
EDS	Energy-dispersive X-ray spectroscopy
$E_g$	Energy band-gap
EIS	Electrochemical Impedance Spectroscopy
FF	Fill Factor
FTO	Fluorine doped Tin oxide
FWHM	Full width at half maximum
HOMO	Highest occupied molecular orbital
$I_{max}$	Maximum current
$I_{sc}$	Short-circuit current
ITO	Indium tin oxide
JCPDS	Joint committee on powder diffraction standards
$J_{sc}$	Short-circuit current density
LUMO	Lowest unoccupied molecular orbital
PEDOT	[poly(3,4-ethylenedioxythiophene)]
$P_{max}$	Maximum power
PV	Photovoltaic
Pt	Platinum

$R_s$	Series resistance
$R_{sh}$	Shunt resistance
SEM	Scanning electron microscopy
TCO	Transparent conducting oxide
$V_{max}$	Maximum voltage
$V_{oc}$	Open circuit voltage
XRD	X-ray diffraction
$\eta$	Power conversion efficiency
$\lambda_{max}$	Maximum absorption wavelength.
FTIR	Fourier Transform Infrared Spectroscopy
PL	Photoluminescence Spectroscopy
KPFM	Kelvin Probe Force Microscopy
AFM	Atomic Force Microscopy
XPS	X-Ray Photoelectron Spectroscopy
UPS	Ultraviolet Photoelectron Spectroscopy
$m_e$	Effective mass of electrons
$m_h$	Effective mass of holes
$\Delta H_f$	Formation enthalpy
A	Electron affinity
$\chi$	Electronegativity
$R_y$	Rydberg energy constant
$\epsilon_s$	Static dielectric constant

# List of Figures

<b>Figure 1. 1</b>	The Band images of n-type and p-type semiconductors (a) before and (b) after joining resulting in a p-n junction. (c) Schematic of a classical sandwich solar cell composed of p- and n-type semiconductors under illumination.....	5
<b>Figure 1. 2</b>	Classification of Solar Cells .....	6
<b>Figure 1. 3</b>	NREL Efficiency Chart for Photovoltaic Technologies .....	11
<b>Figure 1. 4</b>	Three-dimensional cubic perovskite of general formula $AMX_3$ .....	12
<b>Figure 1. 5(a)</b>	Schematic of Conventional Solar Cell (b) Two-dimensional (2D) cross-section of a conventional solar cell. Taken from .....	21
<b>Figure 1. 6</b>	Separation of Light-Generated Charge Carriers .....	23
<b>Figure 1. 7</b>	Schematic diagram of energy levels and transport processes of electrons and holes in an HTM/Perovskite/ETL cell. ....	24
<b>Figure 2. 1</b>	Spin Coating over a Substrate .....	42
<b>Figure 2. 2</b>	Flowchart describing the sample preparation and characterization steps.....	43
<b>Figure 2. 3</b>	Schematic of UV-VIS Spectrophotometer.....	45
<b>Figure 2. 4</b>	Schematic diagram showing Photoluminescence (PL) spectroscopy.....	47
<b>Figure 2. 5</b>	Spectrofluorometer .....	47
<b>Figure 2. 6</b>	Schematic diagram of FTIR Spectrometer .....	48
<b>Figure 2. 7</b>	X-ray diffraction at the sample film surface.....	50
<b>Figure 2. 8</b>	Schematic diagram of Scanning Electron Microscope.....	52
<b>Figure 2. 9</b>	Experimental setup for SEM and EDS measurement.....	53
<b>Figure 2. 10</b>	Working principle of Photoelectron spectroscopy.....	54
<b>Figure 2. 11</b>	(a) Schematic of the Kelvin Probe Force Microscopy (KPFM) testing process. (b) Schematic of the working principle. (c) Topography signal near an embedded nanoparticle. (d) 3D image of the surface topography near an embedded nanoparticle. (e) The DV signal near an embedded nanoparticle.....	56
<b>Figure 2. 12</b>	Setup for I-V measurements .....	57
<b>Figure 2. 13</b>	Equivalent circuit of a solar cell.....	58
<b>Figure 2. 14</b>	Typical I-V characteristics of a solar cell .....	58
<b>Figure 2. 15</b>	Typical QE characteristics of a solar cell.....	62
<b>Figure 2. 16</b>	Experimental setup for EIS measurement .....	62
<b>Figure 2. 17</b>	Typical (a) Nyquist and (b) Bode plot.....	65

<b>Figure 2. 18</b> Experimental apparatus used in the study (a) Weighting scale for precise mass measurements, (b) Ultrasonic cleaner for sample cleaning and preparation, (c) Spin-coater for uniform coating, (d) Hot plate for controlled heating, (e) Solar projector for simulating sunlight exposure.....	66
<b>Figure 3. 1</b> A flowchart that describes an SCF in Wien2k implementation of DFT ...	79
<b>Figure 3. 2</b> Partitioning of the unit cell into atomic spheres (I) and an interstitial region (II) .....	86
<b>Figure 3. 3</b> Program flow in WIEN2k.....	92
<b>Figure 3. 4</b> Device configuration of i-PSC used in the simulation .....	102
<b>Figure 3. 5</b> Input action panel of SCAPS-1D software.....	105
<b>Figure 3. 6</b> Device definition panel.....	106
<b>Figure 3. 7</b> Layer properties panel .....	107
<b>Figure 4. 1</b> Schematic diagram of the fabrication procedure of perovskite photovoltaic cells (a) spin-coating of c-TiO <sub>2</sub> , m-TiO <sub>2</sub> , and Perovskite layer over ITO substrate. (b) Carbon powder deposition. (c) DMSO is injected into the sandwiched cell. (d) spin-coating the mixture of DMSO and Carbon over the perovskite layer.....	118
<b>Figure 4. 2</b> (a)Top view (b)Side view and (c) final setup for I-V measurement of carbon layer-based perovskite solar cell .....	119
<b>Figure 4. 3</b> The SEM images of (a) Pure MASnI <sub>3</sub> thin film (b) DMSO treated MASnI <sub>3</sub> (c) Activate carbon powder (d) Thin film of DMSO and carbon mixture. ....	121
<b>Figure 4. 4</b> FTIR spectra of perovskite and the perovskite/carbon. ....	122
<b>Figure 4. 5</b> (a) UV-Vis's absorption spectra of pure-CH <sub>3</sub> NH <sub>3</sub> SnI <sub>3</sub> film and CH <sub>3</sub> NH <sub>3</sub> SnI <sub>3</sub> with carbon powder layer. (b)-(c) Tauc's plot of the pure-CH <sub>3</sub> NH <sub>3</sub> SnI <sub>3</sub> , CH <sub>3</sub> NH <sub>3</sub> SnI <sub>3</sub> with carbon powder layer to evaluate band gap value. ....	123
<b>Figure 4. 6</b> XRD patterns of (a) CH <sub>3</sub> NH <sub>3</sub> SnI <sub>3</sub> thin film (b) CH <sub>3</sub> NH <sub>3</sub> SnI <sub>3</sub> powder...	124
<b>Figure 4. 7</b> (a) J–V curves and (b) Power-V curves of our fabricated devices under illumination.....	125
<b>Figure 4. 8</b> Energy band diagram of Perovskite solar cell (a) without HTL (b) in the presence of a thin carbon layer .....	126
<b>Figure 4. 9</b> Electrochemical Impedance Spectroscopy analysis of the PSCs (a-c) Nyquist plot along with equivalent circuit (inset) (d-f) Bode plot to identify peak frequency.....	130
<b>Figure 4. 10</b> (a) Partitioning of the unit cell into atomic spheres (I) and an interstitial region (II) (b) Graphical representation of DFT .....	132
<b>Figure 4. 11</b> Cubic Structure of CH <sub>3</sub> NH <sub>3</sub> SnI <sub>3</sub> .....	133

<b>Figure 4. 12 (a, b)</b> Band structure for the cubic phase of $\text{CH}_3\text{NH}_3\text{SnI}_3$ Perovskite <b>(c, d)</b> DOS for Sn, I, and total DOS for $\text{CH}_3\text{NH}_3\text{SnI}_3$ Perovskite calculated by standard PBE-GGA and LSDA method respectively. ....	134
<b>Figure 4. 13</b> Absorption spectra of $\text{MASnI}_3$ using DFT study.....	135
<b>Figure 5. 1 (a)</b> Device architecture of PSC <b>(b)</b> Energy band diagram of the Device. ....	146
<b>Figure 5. 2</b> Optimized Crystal Structure of <b>(a)</b> $\text{CsGeI}_3$ and <b>(b)</b> $\text{CsGeBr}_3$ <b>(c)</b> $\text{CsGeI}_2\text{Br}$ <b>(d)</b> $\text{CsGeIBr}_2$ .....	149
<b>Figure 5. 3 (a-d)</b> The calculated Band Structures, <b>(e-h)</b> total DOS of $\text{CsGeI}_3$ , $\text{CsGeI}_2\text{Br}$ , $\text{CsGeIBr}_2$ , and $\text{CsGeBr}_3$ respectively, <b>(i, j)</b> partial Density of States of $\text{CsGeI}_3$ and $\text{CsGeBr}_3$ respectively. ....	152
<b>Figure 5. 4</b> Relative Investigation of Optical Properties of $\text{CsGeI}_x\text{Br}_{3-x}$ . ....	157
<b>Figure 5. 5</b> Variation of PCE of $\text{CsGeI}_x\text{Br}_{3-x}$ based solar cell with the defect density and thickness of the perovskite absorber layer .....	160
<b>Figure 5. 6 (a)</b> The variations of band gap and $V_{OC}$ <b>(b)</b> Blue-shift of optical properties with different halogen elements from I to Br.....	163
<b>Figure 6. 1</b> Crystal structure of <b>(a)</b> pure <b>(b)</b> Sr/ Cr and <b>(c)</b> Ag/Cu-doped $\text{RbSnI}_3$ , Volume optimization of <b>(d)</b> pure and <b>(e)</b> $\text{RbSnI}_3$ supercell <b>(f)</b> Cu-doped $\text{RbSnI}_3$ .....	179
<b>Figure 6. 2</b> The calculated Band Structures, total & partial DOS of <b>(a, b)</b> Pure $\text{RbSnI}_3$ , <b>(c, d)</b> Cr-doped, <b>(e, f)</b> Sr-doped, <b>(g, h)</b> Ag-doped, <b>(i, j)</b> Cu-doped $\text{RbSnI}_3$ respectively. ....	184
<b>Figure 6. 3 (a)</b> Absorption coefficient and <b>(b)</b> Conductivity for pure and metal-doped $\text{RbSnI}_3$ perovskites.....	187
<b>Figure 6. 4 (a)</b> real and <b>(b)</b> Imaginary parts of dielectric function for pure and metal-doped $\text{RbSnI}_3$ .....	188
<b>Figure 6. 5 (a)</b> Refractive index, <b>(b)</b> reflectivity, and <b>(c)</b> Loss function for pure and metal-doped $\text{RbSnI}_3$ .....	190
<b>Figure 6. 6</b> HOMO-LUMO orbitals of <b>(a)</b> pure $\text{RbSnI}_3$ , <b>(b)</b> Cr-doped, <b>(c)</b> Sr-doped, <b>(d)</b> Ag-doped, and <b>(e, f)</b> Cu-doped $\text{RbSnI}_3$ .....	193
<b>Figure 6. 7 (a)</b> Basic Device diagram <b>(b)</b> Energy band diagram of the device .....	194
<b>Figure 6. 8</b> Simulated J–V curves of <b>(a)</b> Pure, Sr-doped, and Cr-doped $\text{RbSnI}_3$ , <b>(b)</b> Ag-doped and Cu-doped $\text{RbSnI}_3$ <b>(c)</b> QE plot of the simulated devices .....	197
<b>Figure 7. 1</b> Device architecture and the fabrication procedure of $\text{CsSnI}_3$ , $\text{CsSnBr}_3$ , and $\text{CsSnI}_3/\text{CsSnBr}_3$ heterostructure-based perovskite solar cells. ....	212
<b>Figure 7. 2 (a-f)</b> Perovskite layer formation upon heating on a hotplate, where the black color indicates successful perovskite crystallization <b>(g-h)</b> $\text{TiO}_2$ layer before and after	

heating at 450°C (i) CsSnI <sub>3</sub> (dark brown) and CsSnBr <sub>3</sub> (light yellow) perovskite precursor solutions.....	213
<b>Figure 7. 3</b> Crystal structure of (a) bulk CsSnI <sub>3</sub> (b) bulk CsSnBr <sub>3</sub> (c) top view (d) side view of CsSnI <sub>3</sub> /CsSnBr <sub>3</sub> (e) Theoretical XRD patterns of CsSnI <sub>3</sub> , CsSnBr <sub>3</sub> , and CsSnI <sub>3</sub> /CsSnBr <sub>3</sub> heterostructure d) Experimental XRD.....	216
<b>Figure 7. 4</b> SEM and histogram analysis of (a, a') CsSnI <sub>3</sub> , (b, b') CsSnBr <sub>3</sub> , and (c, c') CsSnI <sub>3</sub> /CsSnBr <sub>3</sub> heterostructures (d, d') side view with respective EDS spectra with elemental quantitative data of analyzed elements of CsSnI <sub>3</sub> /CsSnBr <sub>3</sub> .....	218
<b>Figure 7. 5</b> Top-view AFM images of (a, b) the pure CsSnI <sub>3</sub> film and (c, d) CsSnI <sub>3</sub> /CsSnBr <sub>3</sub> heterostructure layer.....	219
<b>Figure 7. 6</b> Calculated band structures of the a) CsSnI <sub>3</sub> _PBE b) CsSnI <sub>3</sub> _mBJ (c) CsSnI <sub>3</sub> _mBJ(001)surface(d)CsSnBr <sub>3</sub> _PBE(e)CsSnBr <sub>3</sub> _mBJ (f) CsSnI <sub>3</sub> /CsSnBr <sub>3</sub> _mBJ. The Fermi level is denoted by a horizontal black dashed line.....	223
<b>Figure 7. 7</b> Calculated TDOS and PDOS: (a) CsSnI <sub>3</sub> _PBE (b) CsSnI <sub>3</sub> _mBJ (c) CsSnI <sub>3</sub> _mBJ (001) surface (d) CsSnBr <sub>3</sub> _PBE (e) CsSnBr <sub>3</sub> _mBJ (f) CsSnI <sub>3</sub> /CsSnBr <sub>3</sub> _mBJ.....	225
<b>Figure 7. 8</b> FTIR spectra of CsSnI <sub>3</sub> , CsSnBr <sub>3</sub> , and CsSnI <sub>3</sub> /CsSnBr <sub>3</sub> heterostructure perovskite.....	226
<b>Figure 7. 9</b> DFT calculated XPS spectra of (a) Cs 3d, (b) Sn 3d, (c) I 3d & Br 3p of CsSnI <sub>3</sub> , CsSnBr <sub>3</sub> , and CsSnI <sub>3</sub> /CsSnBr <sub>3</sub> heterostructure.....	228
<b>Figure 7. 10</b> DFT Calculated optical spectra (a) absorption coefficient, (b) conductivity, (c, d) real & imaginary dielectric function of CsSnI <sub>3</sub> , CsSnBr <sub>3</sub> , CsSnI <sub>3</sub> (001) surface, and CsSnI <sub>3</sub> /CsSnBr <sub>3</sub> heterostructure.....	229
<b>Figure 7. 11</b> UV–Vis absorption spectra and corresponding bandgap of (a, a') CsSnI <sub>3</sub> , (b, b') CsSnBr <sub>3</sub> , (c, c') CsSnI <sub>3</sub> /CsSnBr <sub>3</sub> heterostructure .....	231
<b>Figure 7. 12</b> Photoluminescence emission spectra of CsSnI <sub>3</sub> , CsSnBr <sub>3</sub> , and CsSnI <sub>3</sub> /CsSnBr <sub>3</sub> heterostructure.....	233
<b>Figure 7. 13</b> KPFM images of the (a) pure CsSnI <sub>3</sub> film, (b) CsSnI <sub>3</sub> /CsSnBr <sub>3</sub> heterostructure film, and (c) the corresponding KPFM line scans. ....	234
<b>Figure 7. 14</b> UPS spectrum (a, a'), the cut-off energy ( $E_{\text{cut-off}}$ ) region (b, b'), the Fermi edge ( $E_{\text{F, edge}}$ ) region (c, c') of CsSnI <sub>3</sub> and CsSnI <sub>3</sub> /CsSnBr <sub>3</sub> film .....	236
<b>Figure 7. 15</b> (a) J–V curves, (b) Power-V curves, (c)EQE plots, (d) IQE plots, and (e) the long-term stability of our fabricated devices stored in ambient air without encapsulation.....	240
<b>Figure 7. 16</b> Electrochemical Impedance Spectroscopy analysis of the CsSnI <sub>3</sub> , CsSnBr <sub>3</sub> , and CsSnI <sub>3</sub> /CsSnBr <sub>3</sub> - based PSCs (a) Nyquist plot along with equivalent circuit (inset) (b) Bode plot to identify peak frequency.....	241

## List of Tables

<b>Table 3. 1</b> Input parameters for SCAPS 1D simulation tool .....	103
<b>Table 3. 2</b> Photovoltaic output parameters (functional parameters) of the device ....	104
<b>Table 4. 1</b> Experimental and Calculated Lattice Constants and Direct Bandgaps of Bulk-MASnI <sub>3</sub> .....	124
<b>Table 4. 2</b> Photovoltaic parameters of the fabricated devices .....	126
<b>Table 4. 3</b> The outcome of EIS measurements of PSCs .....	129
<b>Table 4. 4</b> Lattice parameters of light absorber MASnI <sub>3</sub> .....	133
<b>Table 4. 5</b> Comparison of Experimental outcomes with DFT findings.....	136
<b>Table 5. 1</b> Lattice parameters of light absorber CsGeI <sub>x</sub> Br <sub>3-x</sub> .....	150
<b>Table 5. 2</b> The calculated Ge-halide bond lengths of CsGeI <sub>x</sub> Br <sub>3-x</sub> .....	150
<b>Table 5. 3</b> Material parameters used in the simulation.....	158
<b>Table 5. 4</b> The efficiency of the Simulated Device .....	162
<b>Table 6. 1</b> Optimized structural parameters, formation enthalpy ( $\Delta H_f$ ), and tolerance factor ( $t$ ) for <i>Rb1 – kMkSnI3</i> (k = 0.125, M=Cr, Sr, Ag, Cu) halide perovskites ...	181
<b>Table 6. 2</b> The calculated Rb-I and Sn-I bond lengths of pure RbSnI <sub>3</sub> and doped <i>Rb1 – kMkSnI3</i> (k = 0.125, M= Cr, Sr, Ag, and Cu) systems and their ratios .....	182
<b>Table 6. 3</b> Measurement of Exciton Binding energy ( $E_b$ ) .....	191
<b>Table 6. 4</b> DFT-based computed parameters .....	192
<b>Table 6. 5</b> Material parameters used in the simulation.....	196
<b>Table 6. 6</b> The efficiency of the simulated device.....	197
<b>Table 7. 1</b> Optimized structural parameters, formation enthalpy ( $\Delta H_f$ ), and tolerance factor ( $t$ ) for CsSnX <sub>3</sub> (X=I, Br) and CsSnI <sub>3</sub> /CsSnBr <sub>3</sub> halide perovskites compared with the previous study. ....	221
<b>Table 7. 2</b> Measurement of Exciton Binding energy ( $E_b$ ) .....	233
<b>Table 7. 3</b> Energy levels of the CsSnI <sub>3</sub> and CsSnI <sub>3</sub> /CsSnBr <sub>3</sub> films calculated from the UPS and Tauc plots data* .....	236
<b>Table 7. 4</b> Photovoltaic parameters of the fabricated devices .....	237
<b>Table 7. 5</b> The outcome of EIS measurements of PSCs using the equivalent model	242
<b>Table 7. 6</b> Comparison of Experimental outcomes with DFT findings.....	242